

Effect of Externally Applied Transverse Magnetic Field on Unsteady Flow of Blood in Tapered Stenosed Artery



B S Veena

Abstract: *The role of flow parameters of blood is very important in maintaining proper functioning of heart and in turn health body. Herschel–Bulkley fluid model is used for the proposed one-fluid blood flow model. The behavior of important blood flow characteristics wall shear stress, volumetric flow rate and axial velocity of the flow in tapered mild stenosed artery in the presence of externally applied transverse magnetic field is studied. A combination of analytical and numerical methods is used to solve the mathematical model of the system. We report the importance constant/variable viscosity of blood on unsteady flow in the proposed artery. Numerical results are reported for different values of the physical parameters of interest. It is observed with the help of graphs, that the flow characteristics wall shear stress, volumetric flow rate and axial velocity are affected in tapered stenosed artery and flow can be regulated with the help externally applied transverse magnetic field.*

Key words: *Stenosis, Magnetic field, Blood flow, Herschel–Bulkley fluid, Variable viscosity*

I. INTRODUCTION

Atherosclerosis, a major heart disease is one of the most serious diseases which causes death not only in developing countries, but also in developed countries. Atherosclerosis leads to malfunctioning of the cardiovascular system which in turn may lead to stroke, heart attack or even death. The deposition in the inner side of artery, which carries oxygen rich blood to our heart and other body parts, known as stenosis is the initial stage of the disease and this disturbs blood flow. So, study of blood flow is important to understand the fundamentals of circulatory disorders.

In reality, artery is not always cylindrical; it may be tapered, converging or diverging and may bifurcate into branches. Although it may appear like cylindrical in the beginning of bifurcation, it is not in the later parts and also the radius of artery reduces after each bifurcation. The blood flow gets disturbed at each bifurcation and affects the supply of blood to brain and other parts of body. Hence, understanding the behavior of flow characteristics in tapered arteries is essential.

French physician Poiseuille conducted the first experiment to study the flow in capillaries in 1840 and the result is well-known Poiseuille's flow. The first notable work in this area was proposed by Haik et al. [11]. Tzirtzilakis and Kafoussias modified the existing mathematical model of

Haik et al. [18]. It is found, within certain limits, magnetic field lowers shear stress, potency of obstruction at the apex of bifurcation and changes the blood velocity by assuming the flow as incompressible, homogeneous and viscous [17]. Also, in the presence of stenosis, normal flow condition of blood changes to disturbed one causing atherosclerosis [5]. The stress increases with increase in magnetization and increases significantly at higher magnetic field. The pressure gradient increases for both hematocrit and magnetic field but the increase in magnetic field is more significant than that of hematocrit. It is to be noted that the effect of high magnetization is more destructive for diseased cardiovascular system [10]. The rheological behavior of blood is to be somewhat extra complex than behavior of simple fluids. Because of suspended particles in plasma, blood shows anomalous viscous properties [16]. Vessel tapering is one more important factor in blood flow rheology [6]. According to biofluid mechanics, blood does not obey Newton's linearized one parameter law of viscosity. The modeling of non-Newtonian time dependent non-homogeneous blood flow is possible only with the help of higher order equations [8, 9]. The flow rate can be reduced by 40 % if the magnetic field applied is strong enough, which is more as compared to reduction of flow rate in the presence of other types of magnetic field (10%). The flow field can be substantially determined by magnetic field gradient [19]. The behavior of blood flowing through large vessels is different and is Newtonian. This behavior can also be observed in medium and small vessels. But even in large arteries, blood exhibits non-Newtonian behavior in diseased conditions [13]. The flow is substantially influenced by magnetic field and rise in hematocrit level [12]. A study on the outcome of externally applied magnetic field on unsteady blood flow model in non-tapered artery with multiple stenoses showed that magnetic field of different intensities affects all main characteristics of blood flow [20]. It is reported that flow resistance, wall shear stress and effective viscosity decreases with wall slip whereas axial velocity increases [4]. Also, wall shear stress and viscosity decreases as acceleration parameters increases and increases with the increase in magnetization. Further, as magnetic field increases, flow resistance increases. It is also observed that effective viscosity increases as percentage of hematocrit and magnetic field gradient increases. The axial velocity and flow rate decreases slowly magnetic field gradient and hematocrit level increases [3]. The flow characteristics are strongly influenced both qualitatively and quantitatively by yield stress and height of stenosis [15].

Revised Manuscript Received on October 30, 2019.

* Correspondence Author

B. S. Veena, Department of Applied Science, Symbiosis Institute of Technology (SIT), Symbiosis International University (SIU), Lavale, Pune - 412 115, Maharashtra State, India

E - mail: veena@sitpune.edu.in, veena1sreenivasa@gmail.com

© The Authors. Published by Blue Eyes Intelligence Engineering and Sciences Publication (BEIESP). This is an [open access](https://creativecommons.org/licenses/by-nc-nd/4.0/) article under the CC BY-NC-ND license (<http://creativecommons.org/licenses/by-nc-nd/4.0/>)



The magnitude of wall shear stress and its distribution are strongly affected by location, size and other features of stenosis [7, 21]. The model developed throws a light on clinical treatment of such barrier and also helps to reduce at least some complications of coronary thrombosis and ischemia. It also allows simulating and validating different models in different arteriosclerosis conditions. Axial velocity increases as length of stenosis increases [1].

The purpose of this study is to find the role of viscosity in the study of effect of externally applied transverse magnetic field in tapered sensed artery. Blood being a shear thinning liquid, it is not a constant when flowing in an artery (which is in the form of a circular tube) as viscosity of blood is inversely proportional to shear rate. So, variable viscosity of blood which depends on percentage volume of erythrocytes is considered in order to improve resemblance to the real situation. The expressions for wall shear stress, volumetric flow rate and axial velocity are proposed using a combination of analytical and numerical methods and the effect of externally applied transverse magnetic field on these flow characteristics is studied. The exclusive study of effect of yield stress, magnetic field and tapering angle has been carried out, through which the link between biomechanics and arterial disease can be comprehend. Matlab 7.10.0 is used to compute important flow characteristics for different values of parameters. The results are presented in graphs to observe and analyse the effect of magnetic field to control blood flow.

In single-phase model, artery will be considered as one-layered model in which blood behaves in the same way throughout the region. However, viscosity may be constant or it varies with hematocrit.

II. PROBLEM FORMULATION

A tapered stenosed artery which is cylindrical in the beginning and then tapered with tapering angle φ is considered. The geometry of time variant tapered stenosed artery for different tapering angle can be expressed as (in dimensionless form)

$$R(z, t) = \left\{ (R_0 + md) + \left[m - \left(\frac{h}{l} \right) \right] (z - d) + \left(\frac{h}{l^2} \right) (z - d)^2 \right\} a(t)$$

where $d \leq z \leq d + l$

$$R(z, t) = (mz + R_0)a(t) \text{ otherwise [22]} \quad (1)$$

$$\text{where } a(t) = 1 - b(\cos \omega t - 1) e^{-bt} \quad (2)$$

Here $m = \tan \varphi$ where φ is the tapering angle and $h = 4 \tau_m \sec \varphi = 4pR_0 \sec \varphi$, height of stenosis where b is a constant and its value is 0.1 for blood.

Here R_0 is radius of un-constricted non-tapered part of artery, $R(z, t)$ is radius of artery in constricted part, $\omega^* = 2\pi f_p^*$, f_p^* is pulse frequency, φ is angle of tapering, $m = \tan \varphi$, and $h^* = 4 \tau_m^* \sec \varphi = 4pR_0^* \sec \varphi$ where p is a real number between 0 and 1. If $p < 0.4$ then the stenosis is mild, if $0.4 < p < 0.6$ then the stenosis is medium and if $p > 0.6$ then the stenosis is severe.

An unsteady two-dimensional flow of blood in tapered stenosed artery is considered. Artery is considered as one-fluid model; Two cases; (i) constant viscosity and (ii) viscosity varying with shear rate are considered to ascertain

the usefulness of the model in biofluid dynamics. Variable viscosity of blood which is inversely proportional to shear rate which further depends on hematocrit is taken into account for better results.

The different types of tapered stenosed blood vessel are shown in Fig. A. 1. Here φ is tapering angle. If $\varphi < 0$ then the artery is converging, if $\varphi = 0$ then the artery is non-tapered and if $\varphi > 0$ then it is diverging.

The subsequent assumptions have been made to form the problem mathematically; blood is incompressible, non-homogeneous and viscous; flow is two-dimensional, unsteady and fully developed; no induced magnetic field; no external electric field is applied; negligible electric field; transverse magnetic field is applied externally.

The governing equation satisfying all these conditions is given by [2]

$$-\frac{\partial P}{\partial z} + \frac{1}{r} \frac{\partial(\tau r)}{\partial r} + F_1 \frac{dH}{dz} = 0 \text{ where } F_1 = \frac{kMH_0}{\rho u_0^2} \quad (3)$$

Here F_1 is called magnetic number. Magnetic number is a constant which depends on magnetic field. The value of magnetic number increases as magnetization and intensity of magnetic field increases.

Here H^* is intensity of magnetic field, k is magnetic permeability, M is magnetization, τ^* is shear stress and P^* is pressure.

The constitutive equation of shear stress (τ) for core region in which viscosity may vary is given by Herschel-Bulkley model [14].

The dimensionless form of constitutive equation of blood is given by

$$\tau = \tau_0 + \left[F_2 \left(-\frac{\partial u}{\partial r} \right) \right]^{\frac{1}{n}} \text{ if } \tau \geq \tau_0$$

$$\frac{\partial u}{\partial r} = 0 \text{ if } \tau < \tau_0 \text{ where } n > 1 \text{ or } n < 1 \quad (4)$$

$$\text{Here } F_2 = \frac{\mu}{\rho^{n-1} u_0^{2n}} = \frac{\mu_0 [1 + \beta He (1 - (\frac{r}{R_0})^q)]}{\rho^{n-1} u_0^{2n}}$$

$$= F_3 \left[1 + \beta He \left(1 - \left(\frac{r}{R_0} \right)^q \right) \right], F_3 = \frac{\mu_0}{\rho^{n-1} u_0^{2n}}$$

$$\text{and } \mu = \mu_0 [1 + \beta He \left(1 - \left(\frac{r}{R_0} \right)^q \right)] \quad (5)$$

This is valid for dilute suspension of erythrocytes. Here ρ is density, u_0 is velocity of blood, u is axial velocity component and r is radial component.

Here u is axial velocity, μ_0^* = viscosity of plasma = 1.3 to 1.8 cp, He = maximum hematocrit at the centre of artery which normally ranges from 20 % to 50 %, $\beta = 2.5$ for blood, τ_0^* is yield stress which is required to start the flow. Also, n is flow behavior index, when $n = 1$, flow becomes Newtonian. $q \geq 2$ is the parameter determining the viscosity profile for blood. The Einstein's formula (5) is used by assuming blood as dilute suspension of sphere-shaped shape erythrocytes.

The boundary conditions are $u = 0$ at $r = R(z, t)$,

$$\frac{\partial u}{\partial r} = 0 \text{ at } r = 0 \text{ and } \tau \text{ is finite at } r = 0 \quad (6)$$

The values of parameters used to determine the constants F_1, F_2, F_3 and F_4 and to study the profiles of different flow characteristics are given by table B. 1.

III. RESULTS AND DISCUSSION - VISCOSITY IS CONSTANT

A. Axial velocity

Solving (3), (4) and using (6),

$$u = - \int_r^{R(z,t)} \frac{\left(\frac{r}{2} \left(\frac{\partial P}{\partial z} - F_1 \frac{dH}{dz}\right) - \tau_0\right)^n}{F_2} dr \tag{7}$$

Hence,

$$u = - \frac{2 \left(\frac{r}{2} \left(\frac{\partial P}{\partial z} - F_1 \frac{dH}{dz}\right) - \tau_0\right)^{n+1}}{F_2(n+1) \left(\frac{\partial P}{\partial z} - F_1 \frac{dH}{dz}\right)} \text{ where } r \text{ ranges from } r \text{ to } R(z,t).$$

(8)

The expressions for axial velocity is derived as

$$u_c = -2 \left[\frac{\left\{\frac{R(z,t)}{2} \left(\frac{\partial P}{\partial z} - F_1 \frac{dH}{dz}\right) - \tau_0\right\}^{n+1}}{F_2(n+1) \left(\frac{\partial P}{\partial z} - F_1 \frac{dH}{dz}\right)} \right] + 2 \left[\frac{\left\{\frac{r}{2} \left(\frac{\partial P}{\partial z} - F_1 \frac{dH}{dz}\right) - \tau_0\right\}^{n+1}}{F_2(n+1) \left(\frac{\partial P}{\partial z} - F_1 \frac{dH}{dz}\right)} \right] \tag{9}$$

Here r ranges from 0 to R , R is radius of un-constricted part of artery.

Fig. A. 2 depicts the behavior of axial velocity when flow behavior parameter $n = 0.95$ and tapering angles are -0.01 (converging) and 0.01 (diverging). It has been observed that rate of decrease in axial velocity is more when magnetic field gradient is zero as compared to rate of decrease in velocity when magnetic field gradient is non-zero. Theoretically, as magnetic field gradient increases, axial velocity is getting regulated. It can also be observed that the velocity is same (zero) at $r = 1$ in case of converging artery and it is same (zero) at $r = 2$ in case of diverging artery.

If the tapering angles are increased to -0.03 and 0.03 in converging and diverging artery respectively (highly tapered arteries) then the axial velocity decreases very fast when magnetic field gradient is zero in converging artery as compared to diverging artery as shown in Fig. A. 3. It is also observed from Fig. A. 2 and A. 3 that when the tapering angle increases, axial velocity decreases in converging artery and increases in diverging artery.

Fig. A. 4 depicts the profile of axial velocity versus r for different magnetic numbers. It is clear that when magnetic number is small then there is sharp decrease in axial velocity. Axial velocity and its rate of change decreases as magnetic number increases. Further it may be noted that variation in axial velocity is more in diverging artery as compared to converging artery.

B. Volumetric flow rate

Volumetric flow rate is given by

$$Q = 2\pi \int_0^{R(z,t)} r u_c dr + 2\pi \int_{R_c}^{R(z,t)} r u_p dr \tag{10}$$

$$Q = 2\pi \left[\frac{-2 \frac{R^2(z,t)}{2} \left\{\frac{R(z,t)}{2} \left(\frac{\partial P}{\partial z} - F_1 \frac{dH}{dz}\right) - \tau_0\right\}^{n+1}}{F_2(n+1) \left(\frac{\partial P}{\partial z} - F_1 \frac{dH}{dz}\right)} \right]$$

$$+ \frac{4\pi}{\left(\frac{\partial P}{\partial z} - F_1 \frac{dH}{dz}\right)} \left[\frac{\left\{\frac{R(z,t)}{2} \left(\frac{\partial P}{\partial z} - F_1 \frac{dH}{dz}\right) - \tau_0\right\}^{n+3}}{F_2(n+1)(n+3) \left(\frac{\partial P}{\partial z} - F_1 \frac{dH}{dz}\right)} + \tau_0 \frac{\left\{\frac{R(z,t)}{2} \left(\frac{\partial P}{\partial z} - F_1 \frac{dH}{dz}\right) - \tau_0\right\}^{n+2}}{F_2(n+1)(n+3) \left(\frac{\partial P}{\partial z} - F_1 \frac{dH}{dz}\right)} \right] + \frac{2\pi}{F_4} \left[\frac{\left(\frac{R^2(z,t) - R_c^2}{2}\right) R(z,t) \tau_0 - \left(\frac{R^2(z,t) - R_c^2}{2}\right) \frac{R^2(z,t)}{4} \left(\frac{\partial P}{\partial z} - F_1 \frac{dH}{dz}\right)}{\right] - \frac{2\pi}{F_4} \left[\frac{\left(\frac{R^3(z,t) - R_c^3}{3}\right) \tau_0 + \left(\frac{R^4(z,t) - R_c^4}{16}\right) \left(\frac{\partial P}{\partial z} - F_1 \frac{dH}{dz}\right)}{\right] \tag{11}$$

The flowing graphs depict the behavior of flow rate for a range of parameters of interest.

Fig. A. 5 depicts the variation in flow rate in diverging artery ($\varphi = 0.03$) for different magnetic field gradients at $n = 0.95$ and $n = 1.05$. As z increases, volumetric flow rate decreases slowly in the beginning of stenosis and then it increases. After the peak of stenosis, flow rate increases drastically in both the cases when the magnetic field gradient is zero and as gradient increases, rate of change in flow rate decreases and it is almost stable at some point.

Fig. A. 6 shows the behavior of axial velocity in diverging artery ($\varphi = 0.01$) when flow behavior parameter is $n = 0.95$ and $n = 1.05$. In both the cases, it is observed that there is no considerable difference in the behavior of volumetric flow rate. There is no significant change in volumetric flow rate if the angle of tapering is small and if the angle of tapering increases, significant change in volumetric flow rate has been observed in case of $n = 1.05$ and $n = 0.95$.

Fig. A. 7 depicts the behavior of flow rate when $n = 0.95$. In diverging artery, initially the flow rate decreases slowly and then increases drastically. In case of converging artery, flow rate is more in the beginning of stenosis and as stenosis progresses, flow rate decreases and after critical height of stenosis (near the peak of stenosis), flow rate is almost the same irrespective of magnetic field gradient. However it is observed that higher magnetic field gradient slows down rate of change in flow rate.

In Fig. A. 8, the variation in volumetric flow rate is shown for different pressure gradients. It can be noted that as axial coordinate increases from 2 to 4, volumetric flow rate decreases and in the later part, it increases. Also, variation in volumetric flow rate increases as pressure gradient increases. In case of diverging artery, rate of change is less in the beginning and more in the later part which is opposite in case of converging artery.

C. Wall shear stress

The expression for wall shear stress is derived as

$$\tau_w = 2\tau_0 - \frac{R(z,t)}{2} \left(\frac{\partial P}{\partial z} - F_1 \frac{dH}{dz}\right) \tag{12}$$

Fig. A. 9 illustrates the behavior of wall shear stress for different tapering angles in converging and diverging artery. In case of diverging artery, in the beginning, wall shear stress increases slowly and then decreases drastically and in converging artery, it is opposite. In the beginning of stenosis, the difference between wall shear stresses is less with respect to tapering angle and more towards the end of stenosis.

IV. RESULTS AND DISCUSSION – VARIABLE VISCOSITY

A. Axial velocity

Solving (3), (4), (5) and using (6), we get,

$$u = - \int_r^{R(z,t)} \frac{\left(\frac{r}{2}\left(\frac{\partial P}{\partial z} - F_1 \frac{dH}{dz}\right) - T_0\right)^n dr}{F_2 \left[1 + \beta \cdot He \left(1 - \left(\frac{r}{R_0}\right)^q\right)\right]} \quad (13)$$

where r ranges from 0 to R_0

As the integral in equation (13) is an improper integral, Simpson’s 3/8th rule is used to evaluate the integral. The number of subintervals is taken large enough to make sure that this method gives almost exact solution.

It is observed from Fig. A. 10 that as r increases, axial velocity decreases in core region. In case of converging artery ($\varphi < 0$), axial velocity decreases drastically as compared to diverging artery ($\varphi > 0$). It is apparent from the figures that application of magnetic field slows down the variation in axial velocity, through which the blood flow can be regulated.

Fig. A. 11 illustrates the behavior of axial velocity when a) blood is shear thickening ($n > 1$) and b) blood is shear thinning ($n < 1$). As radial component r increases, axial velocity decreases slowly and as pressure gradient increases, axial velocity decreases. Axial velocity will be less when $n = 1.05$ as compared to the velocity profile when $n = 0.95$. The variation in pressure gradient plays an important role in slowing down blood flow.

B. Volumetric flow rate

Volumetric flow rate is given by

$$Q = 2\pi \int_0^{R(z,t)} r u_c dr + 2\pi \int_{R_c}^{R(z,t)} r u_p dr \quad (14)$$

$$Q = -2\pi \int_0^{R(z,t)} r \left(\int_r^{R(z,t)} \frac{\left(\frac{r}{2}\left(\frac{\partial P}{\partial z} - F_1 \frac{dH}{dz}\right) - \tau_0\right)^n dr}{F_2 \left[1 + \beta \cdot He \left(1 - \left(\frac{r}{R_0}\right)^q\right)\right]} \right) dr +$$

$$2\pi \int_{R_c}^{R(z,t)} \frac{r}{F_4} \left[\frac{1}{4} \left(\frac{\partial P}{\partial z} - F_1 \frac{dH}{dz}\right) (R^2(z,t) - r^2) - \tau_0 (R(z,t) - r) \right] dr \quad (15)$$

Since the first part of the above integral is complicated, it is very difficult to evaluate using analytical method. So combination of analytical and numerical methods is used to find volumetric flow rate. As flow rate is increasing or decreasing in a very low phase depending on the values of parameters, it is difficult to differentiate the profile with the help of graphs. The detailed study of volumetric flow rate using two-phase model with variable viscosity is given in

next chapter, hence only some of the results are presented here with the help of tables.

It is observed from the table B. 2 that volumetric flow rate decreases as stenosis progresses in the beginning. In the later part, there is a sharp increase in flow rate irrespective of percentage of hematocrit. However, elevated hematocrit percentage will help in elevating volumetric flow rate.

It can be seen from table B. 3 that flow rate is high in the beginning of stenosis, it decreases till $z = 5$ and then increases slowly. It can also be seen that flow rate increases as time (t) increases and when $t = 0.1$, flow rate attains its lowest value at $z = 5$.

From table B. 4, it is obvious that volumetric flow rate increases as magnetization increases. It can also be noted that flow rate is directly proportional to radius of artery.

C. Wall shear stress

The expression for wall shear stress is derived as

$$\tau_w = 2\tau_0 - \frac{R(z,t)}{2} \left(\frac{\partial P}{\partial z} - F_1 \frac{dH}{dz}\right) \quad (16)$$

Since the wall shear stress doesn’t depend on viscosity, there is no significant change in the profile.

V. CONCLUSION

In this paper, a mathematical model of tapered artery in mild stenosed artery is considered and two-dimensional unsteady blood flow with constant/variable viscosity through tapered stenosed artery is studied by assuming blood follow non-Newtonian path. Blood viscosity is allowed to vary with radial coordinate and hematocrit. Transverse magnetic field is applied externally; suitable governing equation is used. The analytical solutions are presented for volumetric flow rate, wall shear stress and axial velocity. Various combinations of parameters are used to analyze the profile of important flow characteristics. Based on the exhaustive analysis, it is found that tapering angle, viscosity and hematocrit are the important factors influencing the major characteristics of blood. It can be concluded that it is possible to regulate blood flow with the help of proper combination of fluid parameters in tapered arteries with mild stenosis.

REFERENCES

1. Awaludin, I. S., and Ahmad, R. R. (2013). Runge-Kutta method for wall shear stress of blood flow in stenosed artery. *AIP Conference Proceedings*, 1602(1), pp. 240-245.
2. Bali, R., and Awasthi, U. (2012). A Casson fluid model for multiple stenosed artery in the presence of magnetic field. *Applied Mathematics*, 3(5), pp. 436-441.
3. Bali, R., and Awasthi, U. (2011). Mathematical model of blood flow in small blood vessel in the presence of magnetic field. *Applied Mathematics*, 2(2), pp. 264-269.
4. Biswas, D., and Laskar, R. B. (2011). Steady flow of blood through in a constricted artery with body acceleration. *International Journal of Application and Applied Mathematics*, 4(2), pp. 329-342.
5. Chakravarty, S. (1987). Effects of stenosis on the flow-behavior of blood in an artery. *International Journal of Engineering Science*, 25(8), pp. 1003-1016.

6. Chakravarty, S., and Mandal, P. K. (2000). Two-dimensional blood flow through tapered arteries under stenotic conditions. *International Journal of Non-Linear Mechanics*, 35(5), pp. 779-793.
7. Dabagh, M., Vasava, P., and Jalali, P. (2015). Effects of severity and location of stenosis on the hemodynamics in human aorta and its branches. *Journal of The Royal Society Interface*, 53(5), pp. 463-476.
8. Enderle, J., Susan, B. and Bronzino, B. (2000). Introduction to biomedical engineering, London : Academic Press.
9. Fournier, R. L. (1998). Basic transport phenomena in biomedical engineering, Taylor and Francis.
10. Haldar, K. and Ghosh, S. N. (1994). Effects of magnetic field on blood flow through an indented tube in the presence of erythrocytes. *Indian Journal of Pure and Applied Mathematics*, 25(3), pp. 345-352.
11. Haik, Y., Chen, C. J., and Pai, V. M. (1996). Magnetic fluid dynamics of blood flow. *Proceedings of the 11th ASCE Engineering Mechanics Specialty Conference*, pp. 458-461.
12. Jain, M., Sharma, G. C., and Singh, R. (2010). Mathematical modelling of blood flow in a stenosed artery under MHD effect through porous medium. *International Journal of Engineering, Transactions B*, 23(3-4), pp. 243-251.
13. Mandal, P. K. (2005). An unsteady analysis of non-Newtonian blood flow through tapered arteries with a stenosis. *International Journal of Non-Linear Mechanics*, 40(1), pp. 151-164.
14. Misra, J. C., and Shit, G. C. (2007). Role of slip velocity in blood flow through stenosed arteries: a non-Newtonian model, *Journal of Mechanics in Medicine and Biology*, 7(3), pp. 337-353.
15. Nanda, S., and Bose, R. K. (2012). A mathematical model for blood flow through a narrow artery with multiple stenoses. *Journal of Applied Mathematics and Fluid Mechanics*, 4(3), pp. 233-242.
16. Shehawey, E.F.El., Elbarbary, M. E., Afifi, N. A. S., and Mostafa, E. (2000). MHD flow of an elasto-viscous fluid under periodic body acceleration. *International Journal of Mathematics and Mathematical Sciences*, 23(11), pp. 795-799.
17. Suri, P. K., and Suri, P. R.(1981). Effect of static magnetic field on blood flow in a branch, *Indian Journal of Pure and Applied Mathematics*, 12(7), pp. 907-918.
18. Tzirtzilakis, E., and Kafoussias, N. (2001). Mathematical models for biomagnetic fluid flow and applications. *6th National Congress on Mechanics, Thessaloniki-Greece*.
19. Tzirtzilakis, E. E. (2005). A mathematical model for blood flow in magnetic field. *Physics of fluids*, 17(7), pp. 077103.
20. Varshney, G., Katiyar, V., and Kumar, S. (2010). Effect of magnetic field on the blood flow in artery having multiple stenosis: a numerical study. *International Journal of Engineering, Science and Technology*, 2(2), pp. 967-82.
21. Veena, B.S. and Warke, A.S. (2015). Study of blood flow in one half of cosine shaped stenosis in the presence of magnetic field, *International Journal of Experimental and Computational Biomechanics*, 3(2), pp. 121-136.
22. Veena, B. S., and Warke, A. S. (2019). Study of Two-phase unsteady model of blood flow in a tapered stenosed artery in the presence of externally applied transverse magnetic field. *IEEE Xplore*.

AUTHORS PROFILE



Dr. B. S. Veena is working as an Assistant Professor in Mathematics, Department of Applied Science, Symbiosis Institute of Technology, Pune from July 2012. Prior to this, she worked as a faculty in 2-3 reputed Science and Engineering institutes. She did her masters, M. Phil and Ph. D. in Mathematics. Her area of research includes Bio Fluid Dynamics, Mathematical Modeling, Numerical Solutions of PDE and Computational Fluid Dynamics. She attended many faculty development programmes, conferences, presented research papers in conferences and published research articles in peer reviewed journals.

Appendix A

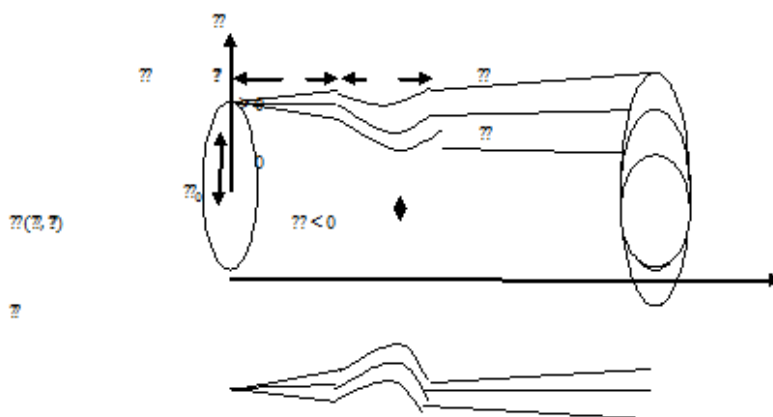


Fig. A.1: Geometry of mild stenosis for different tapering angles with reference to z-axis

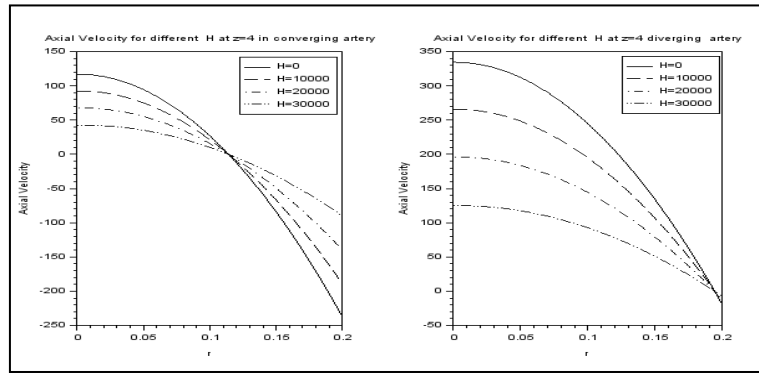


Fig. A.2: Axial velocity for different magnetic field gradients in slightly tapered artery when $n = 0.95$

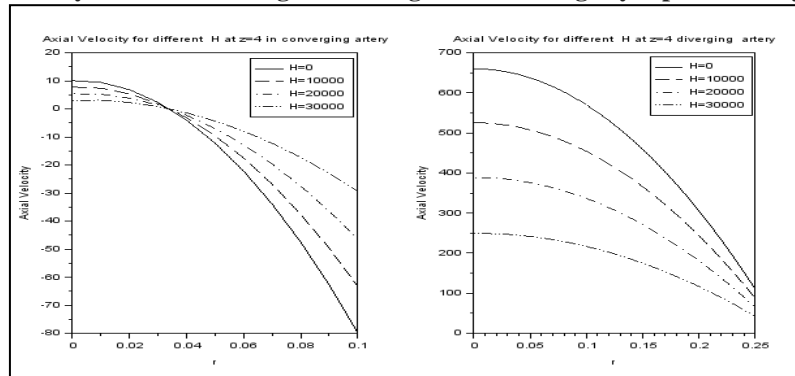


Fig. A.3: Axial velocity for different magnetic field gradients in highly tapered artery when $n = 0.95$

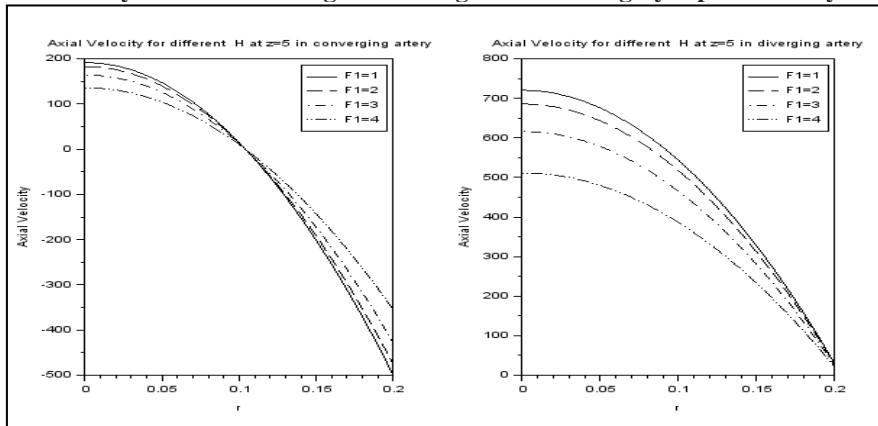


Fig. A.4: Axial velocity for different magnetic numbers in diverging and converging artery

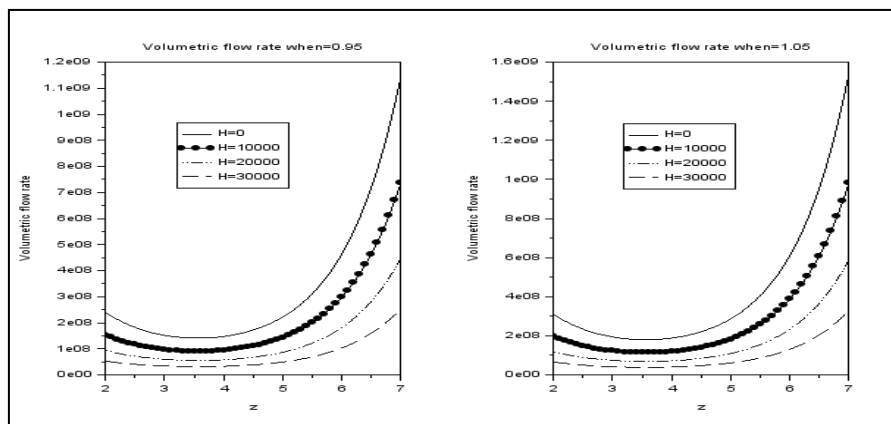


Fig. A.5: Volumetric flow rate for different magnetic field gradients in highly diverging artery

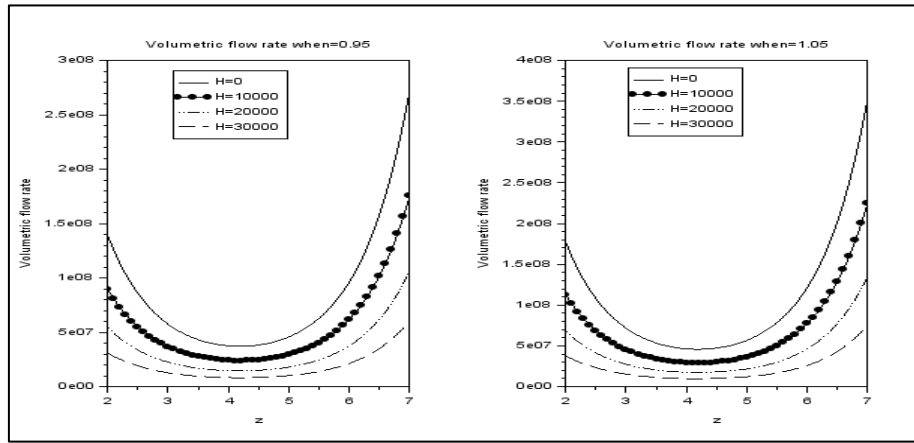


Fig. A.6: Volumetric flow rate for different magnetic field gradients in slightly diverging artery

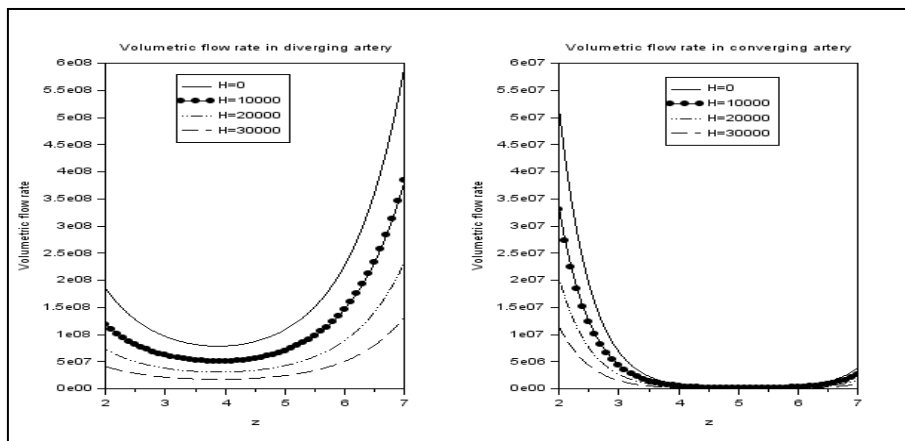


Fig. A.7: Volumetric flow rate for different magnetic field gradients in diverging and converging artery

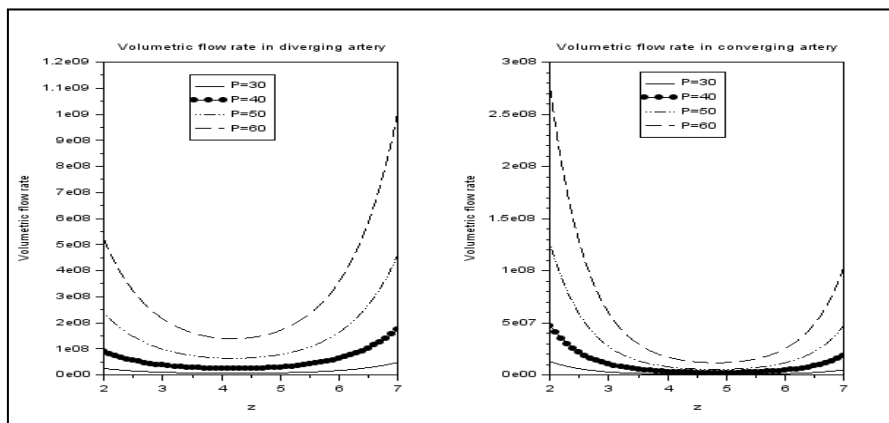


Fig. A.8: Volumetric flow rate for different pressure gradients when $n = 0.95$

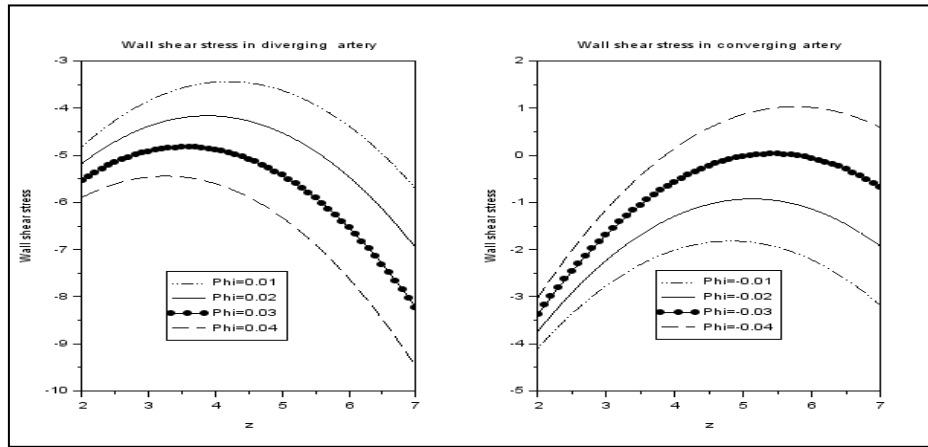


Fig. A.9: Wall shear stress for different tapering angles when $n = 0.95$

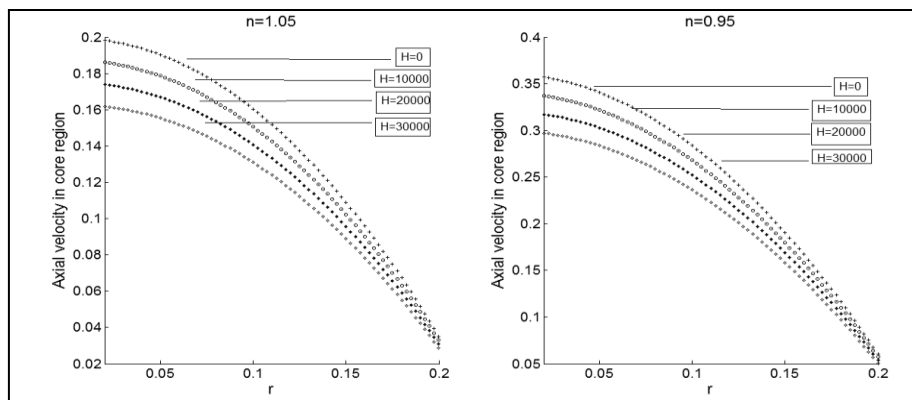


Fig. A.10: Velocity in core region for different magnetic field gradients at $z = 2$ in converging artery

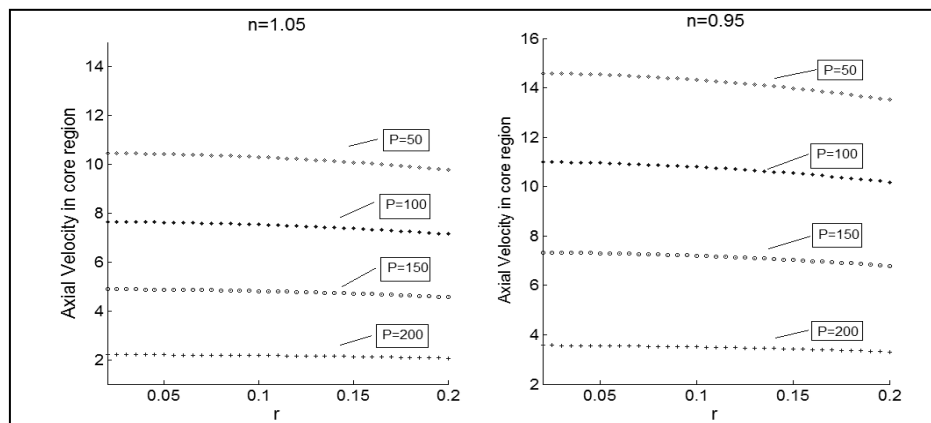


Fig. A.11: Velocity in core region for different pressure gradients at $z = 4$ in diverging artery

Appendix B

Table B.1: Value of various parameters to find F_1, F_2, F_3 and F_4

Parameter	Value	Paramater	Value
μ	3.5 cP	H_0	0.2 Tesla
R_0	0.25 cm	∂	1.06 gm/cm



u_0	36 cm / sec	μ_0	1.5 cP
k	1	M	2 amp / sec

Table B.2: Volumetric flow rate for different values of hematocrit in diverging artery

z	$R(z, t)$	He = 20 %	He = 30 %	He = 40 %	He = 50%
2	0.2700008	1.2957806	1.2971108	1.2981769	1.2990480
3	0.2159979	0.9543090	0.9551738	0.9557716	0.9562643
4	0.1939967	0.8187360	0.8192207	0.8196051	0.8199181
5	0.2039970	0.8797602	0.8803545	0.8808321	0.8812215
6	0.2459990	1.1446732	1.1458069	1.1467327	1.1475068
7	0.3200025	1.5819515	1.5809803	1.5781489	1.5715653

Table B.3: Volumetric flow rate for different time parameters in converging artery

z	$R(z, t)$	$t = 0.1$	$t = 0.3$	$t = 0.5$
2	0.2309962	1.0447694	1.0505606	1.0615996
3	0.1566719	0.6022314	0.6054611	0.6116335
4	0.1144880	0.4004334	0.4022839	0.4058235
5	0.1044443	0.3598746	0.3614361	0.3644233
6	0.1265409	0.4531263	0.4553467	0.4595931
7	0.1807778	0.7385206	0.7426053	0.7504069

Table B.4: Volumetric flow rate for different values of magnetization in diverging artery when $n = 1.05$

z	$R(z, t)$	$M = 2$	$M = 3$	$M = 4$
2	0.2700008	1.2950930	2.3770364	3.4584521
3	0.2159979	0.9550229	1.7130967	2.4710055
4	0.1939967	0.8193188	1.4486400	2.0778661
5	0.2039970	0.8803627	1.5675671	2.2546483
6	0.2459990	1.1449333	2.0836477	3.0220402
7	0.3200025	1.5718832	2.9188796	4.2644306